The Launch Ring – Circular EM Accelerators for Low Cost Orbital Launch

O. James Fiske[*], Michael R. Ricci[†], and Kenneth Ricci[‡]
LaunchPoint Technologies Inc., Goleta, CA, 93117

and

John R. Hull[§]
Argonne National Laboratory, Argonne, IL, 60439

[Abstract] Despite huge potential benefits, no electromagnetic Earth-to-orbit launcher has yet been constructed, primarily due to the difficulty of providing the enormous power required. The Launch Ring adopts circular acceleration and much of the technology of modern synchrotrons to achieve orbital speeds without the need for extremely high power. Superconducting cables and coils are employed to create a passively stable high force magnetic suspension for a maglev "sled", which is accelerated around an enclosed, evacuated circular track of large circumference until it reaches launch speed. A projectile is then released through a tangential exit tube and, potentially, into orbit. Radial accelerations exceeding 10,000 g's and launch speeds exceeding 10 kilometers per second appear achievable with both a relatively small accelerator for launching 10 kg micro-satellites and a larger accelerator for 1000 kg projectiles. Development of Launch Rings could lead to remotely operated assembly facilities in orbit and a radically less expensive approach to space exploitation.

Nomenclature

EM	=	Electromagnetic
ETO	=	Earth-to-orbit
LEO	=	Low earth orbit
LSM	=	Linear Synchronous Motor
NbTi	=	Niobium-Titanium
Nb_3Sn	=	Tri-niobium-tin
YBCO	=	Yttrium, barium, copper-oxide
SCS	=	Superconducting suspension

I. Introduction

Rockets have carried satellites into orbit for almost fifty years now, and this extensive launch experience has made one thing abundantly clear — rocket launch to space will not be inexpensive in the foreseeable future. In fact, there has been little change in the cost to reach orbit for decades[1], and only modest improvements in the cost of rocket launch, at best, are expected anytime soon[2,3]. But the need for low cost space launch is higher than ever.

Electromagnetic (EM) launch has long been considered an alternative that might be capable of providing cheap access to space, prompting numerous investigators to pursue viable launcher designs in the last thirty years. They have been hindered by the difficulty of creating and controlling the immense power required to accelerate a projectile to orbital speed in a short-length linear launcher. Circular accelerators were not considered a viable alternative due to the enormous radial forces that would be generated at orbital speeds in an accelerator ring of

[*] VP Advanced Systems, 5735B Hollister Ave.
[†] VP Engineering, 5735B Hollister Ave.
[‡] Senior Scientist, 5735B Hollister Ave.
[§] Section Manager, Thermal and Electromechanics Section, 9700 S. Cass Avenue/ET-335

reasonable diameter. With the advent of high-current-density superconductors, however, it is now possible to construct magnetic suspensions capable of handling forces of the required magnitude. This presents the opportunity to construct a system capable of launching useful payloads at low cost and with high launch frequency.

The Launch Ring conceptual design is shown in Figure 1. It consists of an enclosed, evacuated circular track of large diameter, in which a maglev "sled" is accelerated to orbital speed.

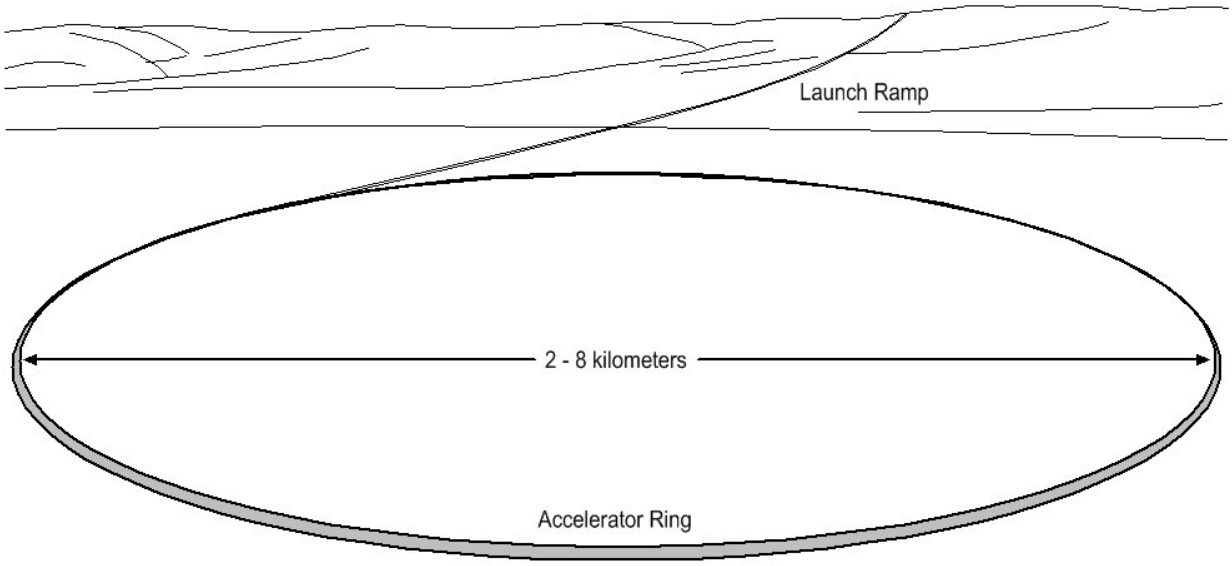

Figure 1. Launch Ring conceptual design

A superconducting maglev radial force compensator provides the sled with both centrifugal compensation and vertical levitation, preventing contact with the passage wall. A projectile is clamped into the sled until it reaches launch speed whereupon the projectile is released into a tangential launch ramp, through an egress hatch and, potentially, into orbit. Multiple sleds and launch vehicles can be accelerated simultaneously.

II. Projectile Design

The projectile design is a critical element of the launch system that must be well understood if the overall system is to be successful — in large part it sets the parameters for the entire system. The goal is not simply to launch objects out of the atmosphere at orbital velocity, but to place these objects into orbit. The projectile must carry the payload, a thermal protection system to withstand hypersonic passage through the atmosphere, a rocket engine and fuel to circularize the orbit, and a control system. Our projectile design was provided by Dr. Miles Palmer of SAIC, a leading researcher in the EM launch field for nearly twenty years, and is shown in Figure 2.

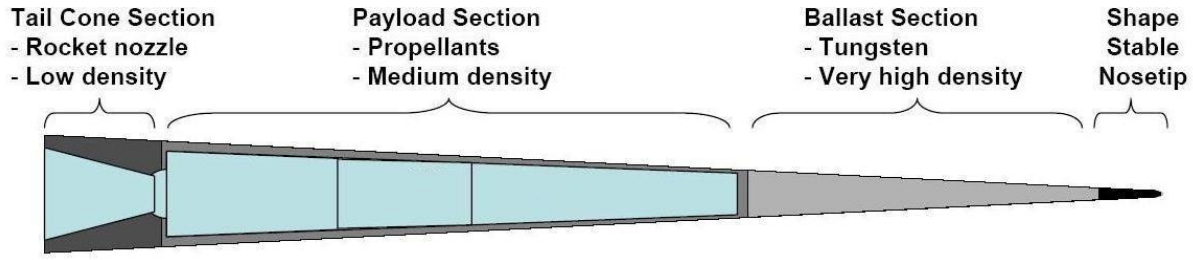

Figure 2. Orbital Launch Projectile Design

Similar projectiles have been described in prior studies[4]. It consists of a conical aeroshell with a non-ablating nose-tip, tungsten ballast, a payload section, rocket fuel, and a rocket, and it uses a hypersonic projectile shape proprietary to SAIC. Ballast ensures that the center of gravity is located forward of the center of pressure, making

the projectile dynamically stable. For our initial design goal of a launch system capable of placing 10 kg micro-satellites into orbit, the projectile would be approximately 3 meters long, with a gross launch mass of 100 kg.

This is a conservative design, emphasizing low risk, with nearly half of the projectile mass in the ballast. Over time, more advanced projectile designs with the ability to maneuver in the atmosphere, similar to the Advanced Maneuvering Reentry Vehicle successfully tested in 1981[5], could be developed. This would allow trajectory changes during atmosphere transit to minimize propellant mass needed for orbital insertion. It would also allow a reduction in ballast. Payload capacity could ultimately reach 40-60 kg without changing gross launch mass.

The projectile must be designed to withstand high lateral force during acceleration and must be highly streamlined. The projectile skin will be constructed of high-strength, high-temperature materials to withstand passage through the first 100 km of altitude. Projectile designs may use transpiration cooling or other related techniques to decrease frictional heating[6], although for large (1000kg) projectiles an ablative carbon-carbon nosetip may prove the most cost effective.

III. Superconducting Levitation

A. Industrial Superconductors

Maglev transportation systems were first proposed nearly 100 years ago, and several large-scale systems have been constructed in the last three decades. The magnetic bearings used in these systems produce levitation pressures on the order of 15 psi (~10 N/cm^2), but it is possible to create far higher levitation force with the type of superconductors now used in particle accelerators.

Figure 3[7] and Figure 4 (A. Ghosh) show the basic capabilities of the NbTi superconducting wire used in the Tevatron particle accelerator. The superconducting state is achieved only when temperature, current density, and magnetic field are all below critical levels. On the graph shown in Figure 3 these three parameters define a "critical surface" – NbTi is in the superconducting state everywhere beneath this surface, and nowhere outside this surface. Figure 4 shows its current carrying capacity vs. magnetic field strength at a temperature of 4.2° Kelvin. Currents of hundreds of thousands of amperes per square centimeter of cable cross section are routinely used with this material.

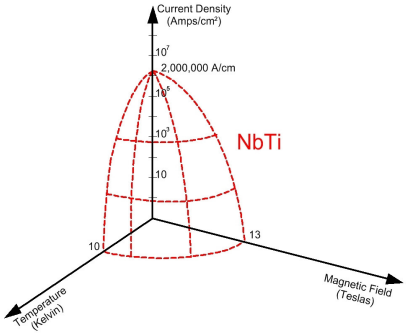

Figure 3. NbTi Critical Surface

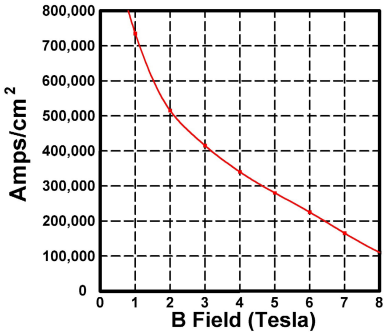

Figure 4. NbTi Current Capability at 4.2°K

As an example of the force levels achievable with this wire, consider two NbTi cables with a gap of 10 cm, center-to-center. The force between the two conductors is:

$$F = \frac{\mu_0}{2\pi}\frac{i_1 i_2}{w} \tag{1}$$

where μ_0 is the permeability of free space ($4\pi \times 10^{-7}$), i_1 and i_2 are the currents in the conductors, and w is the gap width between them. If each cable carries 500,000 amps, the resulting force is 500,000 N per meter of cable.

Magnetic bearings based on this effect are not practical for conventional maglev transportation systems due to high material costs and the requirement for cryogenic cooling on both sides of the bearing. But the technology required is well understood and its potential has dramatic implications for electromagnetic launch. Note that other superconductors such as Nb_3Sn and YBCO far surpass NbTi in current capacity at higher temperatures and field strengths, and so are capable of even higher forces. These superconductors are more expensive than NbTi, thus far, but the high energy physics community is working to bring those prices down to allow their use in particle accelerators.

B. Basic Superconductor Theory as Applied to Levitation Forces

Zero-Field Cooling – Diamagnetic behavior of a superconductor is fundamental to its use in levitation. This is usually best understood by considering a coil geometry. As shown in Figure 5, consider two coils, one above the other, initially without current.

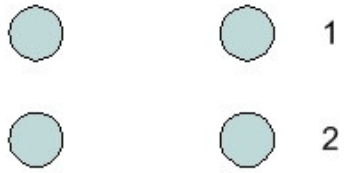

Figure 5. Zero Field Cooling

Let coil 1 be superconducting. Initially, there is no magnetic flux in either coil. Apply a current to coil 2 from an external source. The current in coil 2 produces a magnetic field, as shown in Figure 6, and the flux of this magnetic field penetrates coil 1. Because of Faraday's law, the changing flux in coil 1 produces a voltage that quickly produces a current in coil 1 to keep the net flux in coil 1 at zero. Because the coil is superconducting, the current is persistent. The polarity is shown in Figure **7**.

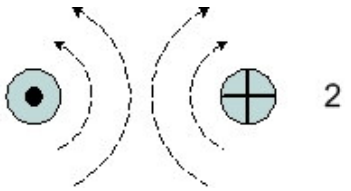

Figure 6. Coil Field

The magnetic field from coil 2, interacting with the induced currents in coil 1 produces an upward force on coil 1. The magnetic field is proportional to current, so the current in coil 1 is proportional to the current in coil 2. The levitation force is proportional to the square of the applied current in coil 2. The process is diamagnetic because the magnetic response of the superconductor is to oppose the applied external magnetic field. The process shown in Figure **5** is sometimes called zero-field cooling, because the superconductor enters the superconductor state when there is no applied magnetic field.

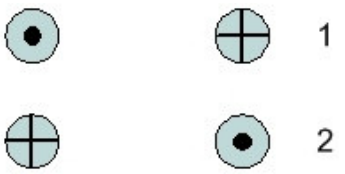

Figure 7. Coil Polarity

Field-Cooling – We can also turn the magnetic field in coil 2 on before coil 1 enters the superconducting state. The initial condition is shown in Figure 8. In this case the magnetic field is present when the superconductor is cooled, and according to Faraday's Law, the superconductor will react to any external changes to maintain this flux. So, for example, if the current in coil 2 is turned off, a current will develop in coil 1 as shown in Figure 9.

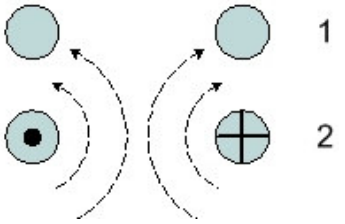

Figure 8. Field Cooling

This affect can be used to advantage to obtain attractive levitation. We start with the situation in Figure 8, where coil 2 is at full current and coil 1 is at zero current. We then decrease the current in coil 2 to half its original value. The current in coil 1 increases accordingly, and is half the value that it reaches in Figure 9. The resulting current polarity in the coils is shown in Figure 10. Comparing the magnetic field produced from coil 2 with the current in coil 1 indicates that there is an upward force on coil 2 — attractive levitation.

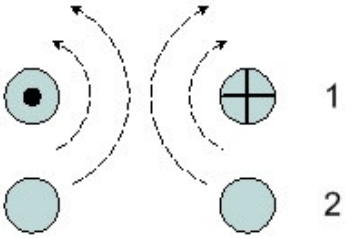

Figure 9. Induced Current

System Stability – In the examples above, we have used changes in the applied current in coil 2 to produce the desired current in coil 1. Changes in coil current may also arise from changes in the separation distance of the two coils, and this can be used to create a statically stable system. In any attractive levitation system, lateral stability is automatically obtained. While permanent magnets in attractive levitation are not stable in the vertical direction, the diamagnetic response of the superconductor can make such a system stable.

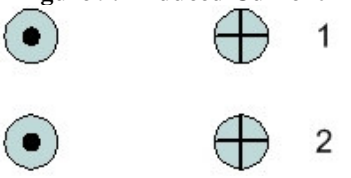

Figure 10. Coil Polarity

Let us consider the arrangement shown in Figure 10 and fix the position and current in coil 1. We assume that there is a downward gravitational or centrifugal force on coil 2 and that the attractive magnetic force exactly counters that force at some equilibrium position. If coil 2 should drift closer to coil 1, then the flux from coil 1 that penetrates coil 2 will increase, and the current in coil 2 will decrease to compensate, thereby decreasing the attractive force. Similarly, if coil 2 drifts further from coil 1, the flux from coil 1 that penetrates coil 2 decreases, and the current in coil 2 will increase to compensate, thereby increasing the attractive force. Thus the system is stable. The actual stability conditions will depend on coil size and spacing.

C. Radial Force Compensation

Repulsive and attractive suspension designs that make use of superconductor characteristics are shown in Figure 11. In the repulsive design, a moving coil is cooled to the superconducting state in a static location within the field of a stationary coil. If the moving coil is then pushed toward the stationary coil, a current develops in the moving

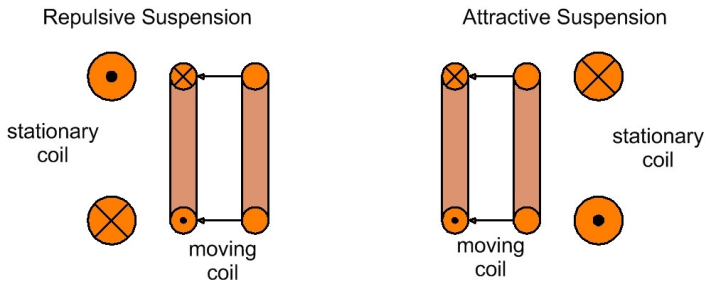

Figure 11. Repulsive and Attractive Suspensions

coil that acts to repel it from the stationary coil and force it back to its starting position. In the attractive design, the moving coil is cooled in a static location near the stationary coil. If the moving coil is then pulled away from the stationary coil, a current develops that acts to pull it back toward the stationary coil to its starting position. These effects can be used to create a "radial force compensator", shown in Figure 12. Here large stationary superconducting coils (stators) are charged with current in the directions shown. In the attractive configuration, small superconducting coils are cooled within the field of the larger coils, and placed in motion around their circumference. As the moving coils increase speed, centrifugal force (inertia) will tend to pull them away from the stationary coil, which will cause currents to develop in the moving coils that will attract them back toward their original distance from the stators. If the speed increases, the separation increases, and the attractive force increases. If the moving coils slow and move closer, their current will decrease and cause the attractive force to decrease. In practice, a single coil is not stable in roll and pitch, so multiple coils must be used. A 4-coil configuration, as shown, is stable in roll, pitch and yaw.

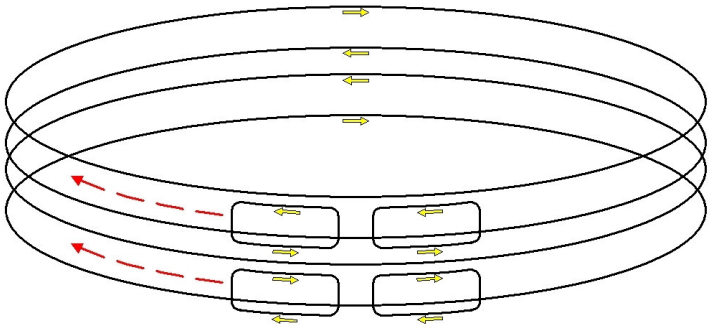

Figure 12. Radial Force Compensator

By taking advantage of the immense current capability of superconductors, and appropriately tailoring the dimensions and inductance of the coils, attractive force can be used to create stable compensation for centrifugal force up to extremely high force levels and speeds. As side benefits, trapped flux provides stable vertical levitation, and the end turns of the moving coils can be used to form the moving elements of a linear synchronous motor. Additional components can be added to the track and sled to dampen vibrations, enhancing stability. Analogously, the repulsive configuration can be used by arranging for the moving coils to orbit inside the stator circumference (on the side closest to the center of the circle).

A different configuration that takes advantage of "shear force" is shown in Figure 13. Here, a moving coil is cooled to the superconducting state in a position just below three concentric stator cables, trapping the flux within the moving coil. The moving coil then begins to orbit the circle, remaining just below the stators. Again, centrifugal force will push the coil outward, causing a current to develop in the moving coil and producing forces (the solid arrows in Figure 13) that will act to return the coil to its original position with respect to the stators. Because the moving coil remains close to the stators, the return forces can be quite large.

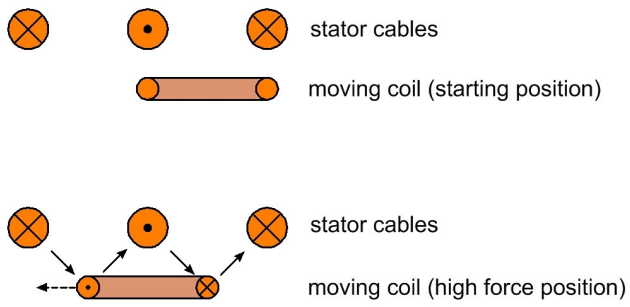

Figure 13. Shear-Force Configuration

Attractive, repulsive and shear force elements can be employed in unison to create a combined superconducting suspension, as shown in Figure 14. A moving element or "maglev sled" is placed in an accelerator tunnel lined with superconducting stator cables. The sled is equipped with multiple superconducting coils, which are cooled to the superconducting state in the static position shown in the left figure. As the sled begins accelerating around the circular tunnel, propelled by a linear motor (not shown), centrifugal force pushes it toward the outer diameter, as

shown in the right figure. All of the superconducting coils on the sled then develop currents that act to oppose any sideways movement. They also provide vertical levitation.

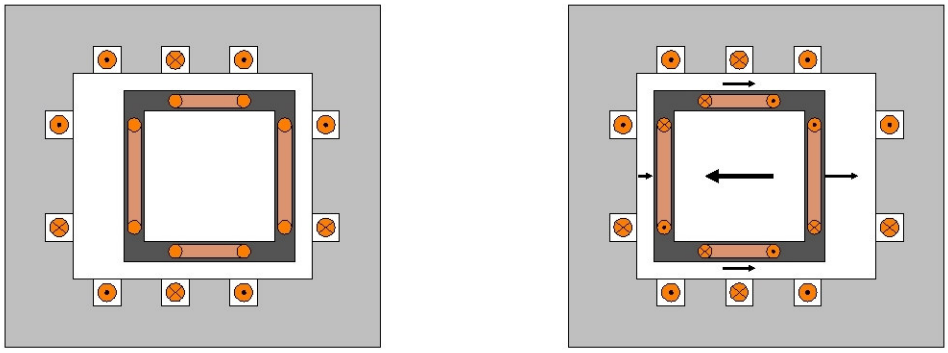

Figure 14. Combined Superconducting Suspension

IV. The Superconducting Suspension (SCS) Launch Ring

A. Superconducting Radial Force Compensator Design.

To determine force capabilities we modeled five superconducting suspension designs: 1) a 2-coil stator with 1 sled coil; 2) a 2-coil stator with 4 sled coils; 3) a 4-coil stator with 4 sled coils; 4) a 6-coil stator with 4 sled coils; and 5) a 6-coil stator with 4 sled coils in a shear-force configuration.

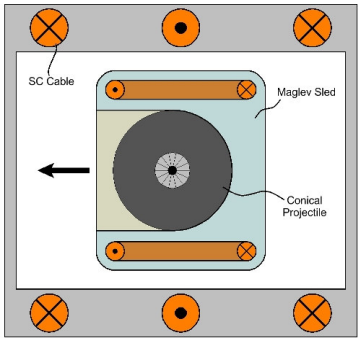

Figure 15. Suspension Model 5

With each succeeding model suspension performance improved significantly, culminating in the Model 5 design shown in the cross-section of Figure 15. The sled has four coils: two on the top (front and back) and two on the bottom (front and back). The stator consists of 6 coils: 3 top and 3 bottom. With this geometry the magnetic field is approximately the same over the entire horizontal traverse of the sled. At zero speed the sled coils are vertically aligned with the 2 right stator coils and coil currents are near zero. As speed increases the sled moves leftward and sled coil currents increase with the polarity shown in Figure 15. Horizontal restoring force from the interaction of the stator and sled coils as a function of sled position is shown in Figure 16, and sled coil current as a function of sled position is shown in Figure 17. These graphs assume the top stator coils are

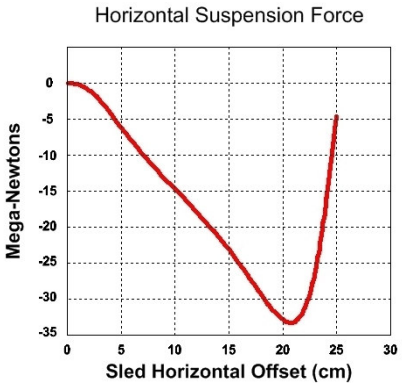

Figure 16. Restoring Force vs. Position

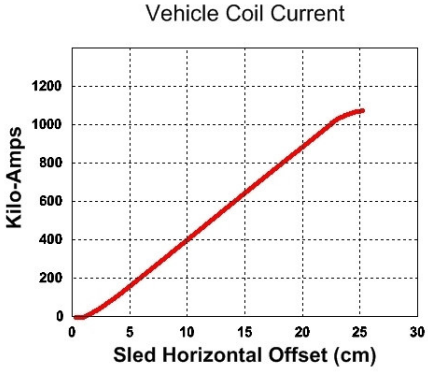

Figure 17. Sled Coil Current

1 meter above the bottom stator coils and stator coil current is 2 x 10^6 amps. Maximum current in the sled coils approaches 9 x 10^5 amps. Peak restoring force is more than 3 x 10^7 Newtons, far exceeding that required for a 200 kg accelerated mass. This configuration is stable in roll, pitch, and yaw and allows ample room for sled rebound when the projectile is released. As a point of comparison, some superconducting magnets now used in particle accelerators carry currents exceeding 6 x 10^6 amps.

Table 1 shows ring diameter and radial g's corresponding to several suspension force levels and an accelerated mass of 200 kg (projectile plus sled). Based on these numbers and the results from Model 5, a ring diameter of less than 2 km appears achievable, if the radial g-forces can be tolerated, depending upon the actual accelerated mass in the final design. Minimum ring diameter is likely to be determined by structural limitations rather than magnetic forces.

Table 1. Ring Parameters

Required suspension force (MN)	5	10	20
Launch Velocity (km/s)	10	10	10
Accelerated mass (kg)	200	200	200
Launch Ring Diameter (km)	8	4	2
Circumference (km)	25.1	12.6	6.3
Radial G's	2,551	5,102	10,204

As projectiles are scaled up they get longer, and restoring force is proportional to the length of the sled coils. The force/current levels of Model 5 would allow the system to be scaled up to far larger projectiles – perhaps 1000kg or more – while maintaining a reasonable ring diameter and cost.

B. Accelerator Structure

A SCS Launch Ring dry lake installation is shown in Figure 18, with breakouts of the accelerator structure, maglev sled, and projectile sabot.

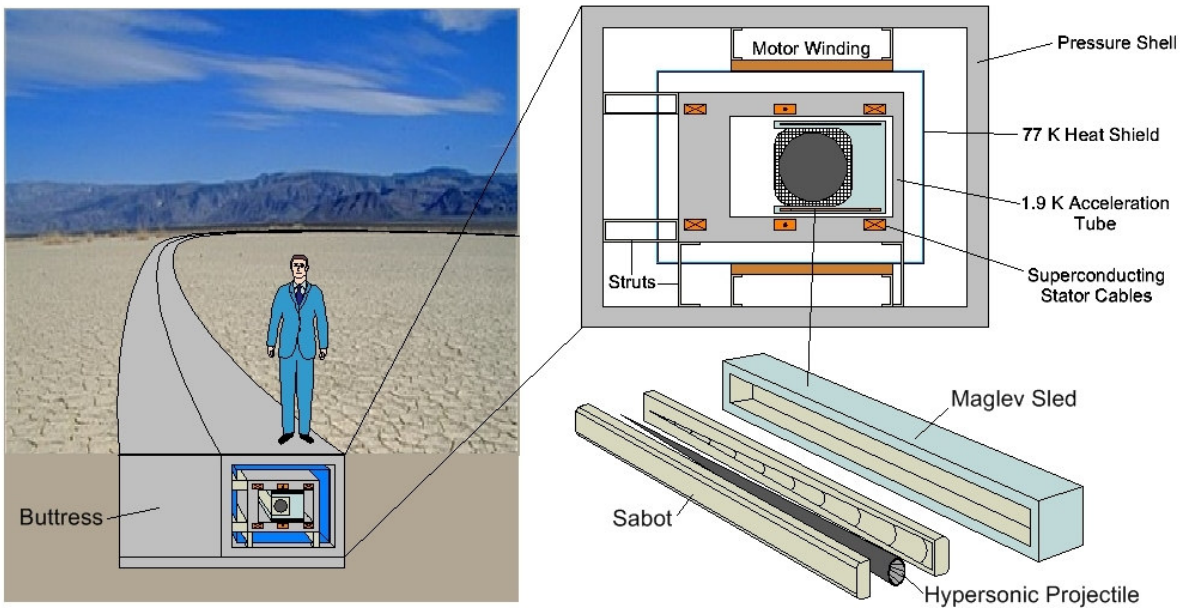

Figure 18. SCS Launch Ring

The accelerator ring is constructed with the top of the ring structure at ground level, and is reinforced by a heavy concrete buttress. The accelerator structure consists of an outer pressure shell, a rough vacuum chamber, a 77K heat shield, a hard vacuum chamber containing the 1.9K acceleration tube with six integral NbTi superconducting stator cables, and a maglev sled with four integral superconducting coils (2 top and 2 bottom). Windings for a linear motor run above and below the acceleration tube, outside the heat shield.

A 200 kg sled (with projectile) traveling 10 km/s in a 2 km diameter ring will exert a periodic force of 2 x 10^7 Newtons at a frequency of 1.6 Hz on the NbTi stator coils. Each meter long section of rail will receive an impulse of 2000 kg m/s when the sled passes. To avoid unacceptable accelerations, the structure supporting the coils against this impulse must weigh many tons per meter. Since it is impractical to enclose such a massive structure in a vacuum

chamber and cool it to 1.9 K, the force will be transmitted by composite fiber struts that extend through the heat shield to the pressure shell. Materials with the highest ratio of strength to thermal conductivity, such as Kevlar, S-glass and carbon fiber composites, are stronger in tension than in compressive loading, but at 1.9K still have compressive stiffness and strength equal to 80% of their tensile strength. This allows the use of a compressive structure design, which is preferable to a tension structure. A preliminary column buckling analysis showed that, for carbon fiber composites, two struts 15 cm long and 2.5 cm thick per 10 megaNewtons of centripetal force will provide sufficient strength to support the stator cables while the sled passes at full speed. These struts will conduct 0.25 watts of heat per cm thickness per meter of rail length to the liquid helium cooled stators, or about half that equivalent heat load when the struts are cooled by heat intercepts carrying 5-10 K helium gas. This is the primary heat load on the helium cryoplant, and is similar to previously built helium cooling systems, such as the CERN LHC helium cryoplants that handle an 18 kW heat load at 4.5 K. The estimated cost of large-diameter fiber-reinforced polymer vacuum pipe and large-volume concrete buttressing is less than $10 million for a Launch Ring with 1000 meter radius.

C. Eddy Currents and Materials Concerns

Large vacuum chambers are usually built of stainless steel for high strength and good surface qualities, but a sled with high magnetic fields passing near a stainless steel pipe can induce large eddy currents and unacceptable drag or heating. This effect will be greatly reduced if the vacuum pipe and other non-superconducting structures near the sled use non-conducting materials such as ceramics, glass or carbon composites, or concrete reinforced with fiber composites. The pipe will be coated with glass or a ceramic glaze to provide a non-porous surface for high vacuum pump-down. The heat shield, however, must be surfaced with electrically-conductive material to achieve high reflectivity and low emissivity over the full spectrum of thermal infrared emission. Eddy currents can be reduced by making heat shield structural components of non-conducting material, coated in the same manner as the vacuum pipe. A 1-micron aluminum layer coated onto the heat shield in a checkerboard-pattern will reflect over 95% of the incident radiation while still limiting eddy currents. The beams supporting the stator coils and coolant pipes will also be non-conducting. Non-superconducting wires such as the copper stabilizer encasing the NbTi superconductor (for quench protection) will use Litz-wire type construction to minimize eddy-current loops.

D. Sled Aerodynamic Heating During Acceleration

One concern is that aerodynamic heating during the extended acceleration period will increase sled temperature to such an extent that the cryogenic environment required by superconductors in the sled cannot be sustained. To determine if this is the case, earlier work performed by John Hull at Argonne National Lab[8] was used to provide a starting point for determining actual sled and projectile aerodynamic heating. The acceleration tube design is cooled to 1.9 K, similar to a synchrotron particle accelerator. At 10^{-11} atmospheres (a level routinely used in particle accelerators) and a speed of 10^4 m/sec, aerodynamic heating is 0.2w/m^2 of skin surface. Heating scales directly with velocity squared and with the density of the gas. Using the Stefan-Boltzmann constant ($\sigma = 5.67 \times 10^{-8}$ W/m^{2}K^4), and a surface emissivity (ε) of .94:

$$Q/A = \text{heat radiated in watts/m}^2 = \sigma \varepsilon (T1^4 - T2^4) \quad (2)$$

Table 2 shows heat radiated at various sled skin temperatures. If the sled skin temperature climbs above 44 K, heat radiation will exceed the 0.2w/m^2 maximum caused by aerodynamic heating, even at a speed of 10^4 m/sec, preventing further temperature rise. With a high temperature superconductor such as YBCO used for the sled coils, operating temperature may even be above 44 K, eliminating any heating problem entirely. Sled insulation and/or a phase-change cooling material such as solid Neon would maintain lower coil temperatures over the course of the acceleration period, allowing the use of low temperature superconductors in the sled coils. The 1.9 K temperature of the acceleration tube will also serve as a cryogenic pump to reduce air pressure even further, and make aerodynamic heating unlikely to prevent effective system operation.

Table 2. Sled Heat Radiation

Sled skin temp (deg K)	10	20	30	40	44	50	60	70
Emissivity of radiator	0.94							
cold shield temp (deg K)	1.9							
Heat radiated (w/m^2)	0.001	0.009	0.043	0.14	0.20	0.33	0.69	1.28

E. Projectile Release

The primary sequence of events at projectile release are illustrated in Figure 19.

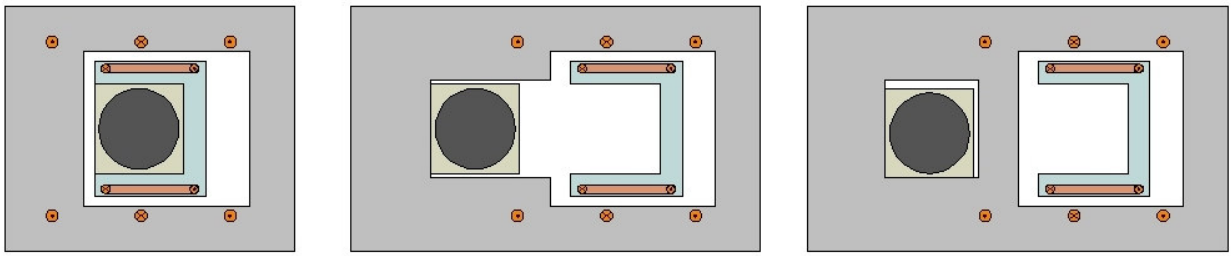

Figure 19. Projectile Release and Ring Bifurcation

In cross-section A, the sled is traveling at launch speed with a narrow gap between it and the outer acceleration tube wall. As the sled approaches the launch ramp, the projectile and sabot are released from the sled. The projectile moves tangentially to the ring, so it travels a significant distance forward before contacting the wall. Assuming the sled is moving at 10 km/sec at the release point, and projectile-to-wall separation is 5 mm just before release, the projectile will contact the wall with a radial speed of 15.8 m/sec, equivalent to a free-fall in one gravity from a height of 12.8 meters. Impact is cushioned by compressible material in the sabot, with the remaining shock easily handled by the projectile, which must be designed to withstand in excess of 2000 g's during the acceleration period.

As the projectile and sabot slide along the wall, Lexan ablation creates a gas bearing[9], preventing excessive speed loss or damage to the projectile. In cross-section B, the launch ramp has begun to separate from the acceleration tube. In C, the launch ramp is fully separated from the acceleration tube and the projectile is a fraction of a second away from the launch ramp exit.

F. Sled and Sabot

The sabot around the projectile will be comprised of high strength-to-weight ratio carbon fiber composite with a hollow-core or honeycomb type of structure and Lexan ablation surfaces in required areas. The projectile and sabot will be held in the sled using a thin Kevlar sling. At the release point in the Launch Ring, a laser knife will slash open the sling along two lines – assisted by pyrotechnic cords in the sling – allowing the projectile and sabot to separate from the sled and enter the launch ramp. From friction data on hypersonic projectile tests in steel tubes[9], we estimate that a 100 kg projectile will ablate 10-40 kg of Lexan as it traverses a 500 meter long steel launch ramp into a 30° launch trajectory at a speed of 10 km/second. Ablation can be minimized by placing an air-scoop on the sabot to force low-pressure gas in the launch tube underneath the projectile, increasing gas bearing pressure and decreasing projectile friction.

In an initial point design, the sled is envisioned as a hollow rectangular prism 330 cm long by 50 cm square, holding the conical projectile in a cylindrical sabot. One side of the sled is open, except for the Kevlar sling, for projectile release. The other five walls of the box will be made of hollow-core or space-frame carbon fiber composite members to provide maximum strength and stiffness with minimum mass. Stiffener plates will encircle the inside half of the sabot to provide the required rigidity to the midsection of the open box frame. With a design strength safety factor of 4, the combined frame and Nb_3Sn coil mass would require 230 kg of material to withstand a centripetal force of 30 MegaNewtons. With a 100 kg projectile and 30 kg sabot at launch velocity 10 km/s, this corresponds to a Launch Ring 1200 meters in radius.

G. Linear Motor

Sled propulsion would be provided by a 3-phase centrally-controlled linear synchronous motor (LSM) with "zigzag" stator windings that extend around the entire ring. The stator windings interact with the magnetic fields of the superconductor suspension coils on the sled that form the "rotor" and excitation of the motor system. At the start of sled acceleration, however, very little current is flowing in the sled suspension coils since this current is related to centripetal force. With only the resulting weak field to grapple, a 10 MW linear motor would require roughly 10 hours to accelerate the sled to launch speed. To improve performance, superconducting motor coils can be built into the sled, as shown in Figure 20, and charged with 200kA before acceleration begins.

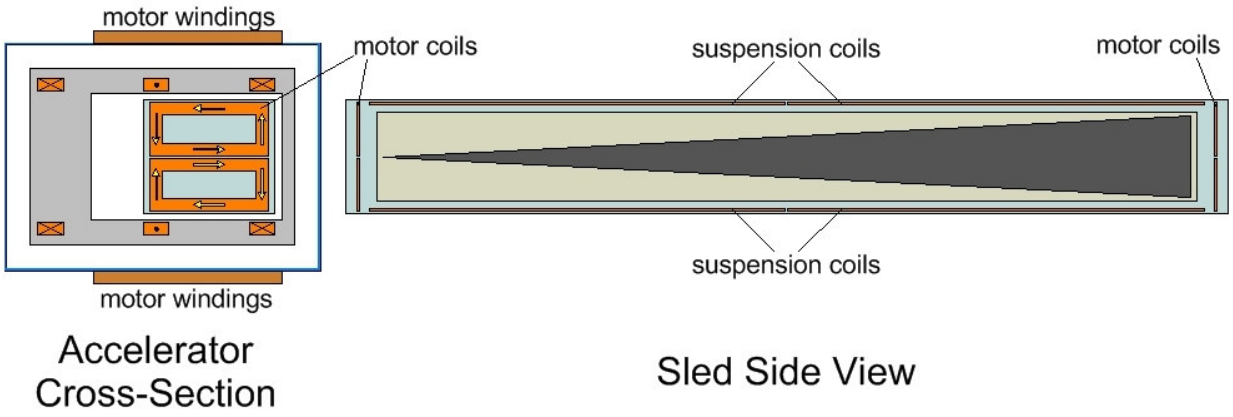

Figure 20. Sled Motor Coils

The resulting high fields from the sled coils make the motor extremely effective, even with a relatively large gap, so the stator windings can be located outside the vacuum chamber to allow air cooling and separate the motor heat load from the cryogenic cooling system. It also allows for easy assembly, maintenance, and repair of the stator coils. Motor windings are constructed of copper Litz wire to maximize current capacity at the high frequencies required and to minimize eddy currents induced in the motor stator as the sled passes at high speed.

To reduce power dissipation the stator is divided into approximately 30 sections, with the specific number depending on the ring circumference chosen for the final design. Two sections are powered at any one time, with semiconductor switches to energize/de-energize the feeder lines to each section. The motor requires an electronic drive to synthesize the 3-phase stator currents from startup to launch.

Based on a preliminary analysis, using just the sled motor coils as the "handles" and ignoring the field contribution of the sled suspension coils, a motor with 2.5 MW power output will accelerate the sled to 10 kps in roughly 4700 seconds (78 minutes). Peak I^2R losses in the motor are 230 kW, with a further loss of 800 kW in the feeder lines from the central drive to the active motor sections. The cost of motor copper is approximately $2.1M, plus another $4.3M for copper in the feeder lines. Motor current starts at 3800 amps, and begins to taper off when the motor output reaches 2.5 MW. As the motor frequency continues to climb, motor output power remains constant at 2.5 MW. Motor back EMF peaks at 700 V, and peak motor frequency is 2500 Hz. 3.5MW motor drive electronics will cost in the range of $3.5M to $7M, bringing the total cost of motor components to approximately $15M.

A motor efficiency of approximately 70% (not including power electronics) can be expected at peak speed, using basic assumptions about the costs of semiconductors and the tradeoffs of motor copper cost versus power efficiency. This figure could be improved by adding copper to the stator and feeders, at additional cost.

As sled speed increases, current in the sled suspension coils steadily increases as well, as described previously. From Faraday's Law, increasing magnetic fields from the sled suspension coils will cause the current in the sled motor coils to decrease, but eventually the fields from the suspension coils will be much larger than the initial motor coil fields. This additional excitation at high speed will increase back EMF in the linear motor and allow a reduction in motor current and I^2R losses or a reduction in copper costs. The precise effects have not yet been calculated.

The feeder structure could be improved over the "30 spoke wheel" design, reducing feeder cost by as much as a factor of two while only slightly increasing I^2R losses. Motor and feeder costs are based on the bulk cost of copper Litz wire, but with a peak frequency of only 2.5 kHz the feeder lines can probably use a lower cost high voltage/low inductance cable structure. Motor fabrication and stator support structure costs have not yet been estimated.

H. Cryogenic and Vacuum System

The cryo and vacuum system takes advantage of similar designs developed for superconducting particle accelerators over the last several decades[10]. The rough vacuum chamber is 10 cm wide and filled with super-insulating ($7x10^{-4}$ w/m-K) glass microspheres that conduct 14 times less heat than the 300K radiation that would cross a vacant gap the same width, reducing the load on the liquid N_2 system. Microsphere insulation is 20 times cheaper than the equivalent cryoplant, but would not be as effective inside the 77K heat shield, which emits 230 times less radiation than do 300K surfaces. Thus, the vacuum system is divided into two regions, the rough vacuum (10^{-6} atm) chamber filled with microspheres, and a high vacuum chamber (10^{-11} atm) enclosed by the heat shield. Liquid nitrogen is pumped through small channels to cool the heat shield, which is coated with a 1μm thick, low-

emissivity aluminum reflector to minimize IR heat transfer. The heat shield also serves as a fiberglass high-vacuum tube with low temperature preventing epoxy resin in the fiberglass from outgassing into the high vacuum space. The heat shield cross-section is rectangular instead of circular, to allow the non-superconducting motor windings to be outside the heat shield but as close as possible to the sled coils they accelerate. The heat shield structure itself can be very thin since the spaces on both sides will be evacuated, leaving no mechanical pressure.

The primary heat load to the 1.9K space is through the fiber composite struts that hold the accelerator tube. This thermal load is small, and can be reduced by roughly another factor of 2 by using the return gas from the liquid helium system lines at 5-10K to intercept the heat in the struts half-way between the heat shield and the superconducting rails, as demonstrated in the Large Hadron Collider particle accelerator design. The resulting cryoplant cost estimates for a Launch Ring with 1000 m radius are in the $30 - $50 million range.

I. Superconductor Quench

Superconductors are sensitive to AC fields, a problem encountered in the Japanese MLX-01 maglev train[11], which initially used low temperature superconducting NbTi coils in the vehicles. Fluctuating magnetic fields produced by the interaction of the high-field vehicle coils and discrete levitation coils in the track caused the vehicle coils to quench, i.e. leave the superconducting state, which of course could cause catastrophic de-levitation if it happens at high speed. The developers solved the problem by replacing the NbTi superconductors in the vehicles with YBCO superconductors, which operate at a higher temperature and are much more resistant to quenching.

In the SCS Launch Ring design, quenching in the sled coils is not the issue of concern – they experience primarily DC fields produced by the stator cables and a nearly constant field in the form of a traveling wave from the linear motor. The potential problem is quenching in the stator cables themselves due to fluctuating magnetic fields caused by rapid passage of the maglev sled. The frequency of the field fluctuation experienced by any particular segment of the stator cables is far lower than that caused by the MLX-01 track coils, but the flux is higher. The frequency may be low enough that quench is not a problem, but that will remain uncertain without more detailed study. If necessary, the threat of a quench could be considerably reduced using the same method used in the MLX-01, i.e. high temperature superconductors.

J. Environmental and Safety Issues

As the projectile exits the launch ramp at 8+ km/second, it will create what could be a substantial shockwave zone, depending upon the size of the projectile and the launch angle. This, along with range safety, will require that the Launch Ring be constructed in a remote location. Conventional missile-launch safety protocols will be required, including the capability to destroy projectiles that malfunction and threaten to deviate from acceptable launch trajectories.

A further safety issue involves the Launch Ring itself. The ring, the projectile, and the maglev sled must all be designed such that a malfunction during acceleration is unlikely to result in severe damage to the ring. This can be accomplished through the use of back-up ablative bearings, emergency braking, and “dump tubes” – tangential branches off the ring where the projectile and sled can be redirected if necessary. The projectile and sled would be destroyed, but the ring would remain intact.

K. Projectile Cost Estimates

Projectile costs may be derived using standard flight vehicle cost estimation techniques. Based on a long history of air vehicle development, a projectile of the type needed by the Launch Ring is expected to cost approximately $300 per pound of vehicle dry weight[12] for the initial production prototypes. For a gross launch weight of 1000 kilograms the projectile will have an empty weight of about 300 kilograms, giving an initial cost of $198,414. As production quantities increase this cost will drop according to established learning curves. Table 3 shows the result of applying an 85% learning curve to the projectile cost for quantity production. Larger production volumes will decrease cost further. Costs may also decrease if, in some applications, we are able to re-use projectile components such as avionics.

Table 3 1000-kg Projectile Production Cost

N (Number of units built)	1	10	100	1,000	10,000
Projectile dry weight (kg)	300				
Payload (kg)	600				
Cost of Nth unit	$198,414	$140,466	$99,443	$70,400	$49,839
Cost/lb of payload	$150	$106	$75	$53	$38

L. Operating Cost Estimates

Using projectile cost estimates and very preliminary estimates of construction cost, we can roughly estimate the most important number of all – the cost to launch a payload to LEO. Table 4 factors in the primary contributors to calculate projectile launch costs for 300 to 3,000 shots per year, assuming a projectile gross weight of 1000 kg and a payload of 600 kg.

Table 4. 1000-Kg Projectile Estimated Launch Costs

Shots/year	300	3,000
Launch Ring capital cost ($M)	$500	$500
Projectile mass (kg)	1,000	1,000
Payload mass (kg)	600	600
Energy usage (kWh/kg)	12.5	12.5
Energy cost ($/kWh)	$0.05	$0.05
Cost of projectile ($k)	$100	$70
O&M costs (% of cap cost)	10	15
Energy cost/shot ($)	$625	$625
Projectile costs/year ($M)	$30	$210
Amortization cost/yr ($M)	$54	$54
Energy costs/year ($M)	$0.2	$1.9
O&M costs/year ($M)	$50	$75
Total costs/year ($M)	$134	$341
Total costs/shot ($)	$447,292	$113,625
Projectile fraction of cost	0.22	0.62
Cost/kg of payload ($)	$745	$189
Cost/lb of payload ($)	$338	$86

This example assumes construction is commercially capitalized, with amortization (at 7% simple interest per year) included in the launch costs. At a launch rate of 3000 shots per year, the resulting cost of $86 per pound is far lower than any other known or expected launch technology. At higher rates the cost drops even more. Note that the majority of the total launch cost at high launch rates is due to the cost of the projectile (Projectile fraction of cost). This tells us two important things: 1) any unexpected projectile cost reductions resulting from as-yet undiscovered technologies, improved manufacturing techniques, or component re-use will quickly bring launch costs even lower; and 2) at high launch rates the launch cost is relatively insensitive to the construction cost of the accelerator ring.

M. G-Hardened Payload Design

High-g tolerant structures and electronics have been in use for at least three decades. The Copperhead 155mm laser-guided artillery round has been in Army service since 1980. Precision guided munitions of this kind typically experience gun shocks of 10,000 to 20,000 g's. Future gun-launched applications will encounter in excess of 20,000 g's[13]. Improving materials and fabrication techniques now permit more intricate systems, including small drone aircraft[14], to be developed for gun launch. High-g spacecraft designs for gun or electromagnetic launch have also been proposed[15]. Many of these designs will be applicable to Launch Ring payloads, with one significant change — the g-loading is much lower. Instead of 10-20 thousand g's or more the forces could be five thousand g's or less, depending upon ring diameter. Furthermore, the g-loading is transverse (across the short dimension) rather than axial (along the long dimension) as in gun launch, easing design constraints. Elements such as folding antennae, mirrors, airfoils, or inflatable structures will be much less difficult to implement.

Some of the economic issues involved in the comparison between a few large, low-g payloads and many small, high-g payloads are examined in reference 16. Greatly reduced launch costs for the small, high-g payloads can give them a major advantage in some applications, even when the increased cost of g-hardening is considered. This is particularly the case when an application can utilize many identical copies of a single payload design, as with constellation satellites.

N. Implications for Human Activities In Space

For every person launched into orbit – or beyond – many tons of oxygen, fuel, food, water, components, construction materials and radiation shielding will be needed. Nearly all of this materiel could be shipped via Launch Rings, resulting in major reductions in the cost of manned space activities. This is only the beginning.

Launch Rings could be used to ship components and materials to space facilities where remotely operated robots, with their operators located in comfortable offices on the planet surface below, could assemble and test equipment and facilities for use in space. Additional assembly robots, test equipment, and facility space along with communication, imaging, and radar satellites of unprecedented capability, vehicles for transport to higher orbit, solar energy collectors, space and planetary exploration vehicles, and many other products are candidates for assembly — essentially anything that can be assembled from G-tolerant subassemblies, components and materials. NASA has done extensive development of telerobotics[17], and telerobots are already being used in the medical field for remote surgery. Remote assembly is arguably an easier task. Using this approach, the cost to establish and maintain a major support infrastructure in space could be radically reduced relative to the currently expected cost.

V. Conclusions

Circular electromagnetic launch accelerators offer a promising new approach to low-cost space access. Preliminary analysis has revealed no insurmountable technical obstacles to construction of an operational system, and suggests the possibility of launch costs below $100/lb to LEO. In combination with the emerging technology of telerobotics, this launch capability could lead to vastly expanded human activities in space in the near future.

Acknowledgments

This research was supported in part by the U.S. Air Force Office of Scientific Research under Contract no. FA9550-05-C-0111.

References

[1]B. D. Watts, "The Military Use of Space: A Diagnostic Assessment", report by the Center for Strategic and Budgetary Assessments, February, 2001

[2]A. Turner, "Aquarius", AIAA 2000-5284, AIAA Space 2000 Conference, 21 September 2000

[3]Interview with Elon Musk on *The Space Show* , May 31, 2005

[4]H. D. Fair, P. Coose, C. P. Meinel, D. T. Tidman, "Electromagnetic Earth-To-Space Launch", *IEEE Transactions On Magnetics*, Vol. 25, No. 1, January 1989

[5]R. A. Hartunian, "Ballistic Missiles and Reentry Systems: The Critical Years", *Crosslink* (the Aerospace Corporation magazine) Volume 4, Number 1 (Winter 2003)

[6]W. H. Kinare, "Feasibility of Nose-Cone cooling by the Upstream Ejection of Solid Coolants", NACA Research Memorandum, Washington, March 1958

[7]T. Shintomi, *Superconducting Magnets for High Energy Particle Accelerators*, June, 2000

[8]J. R. Hull, M. K. Iles, "Magnetically Confined Kinetic-Energy Storage Ring: A New Fundamental Energy-Storage Concept", ANL-84-19, Argonne National Laboratory, Argonne, Illinois, February, 1984

[9]D. A. Tidman, "Slingatron: A High Velocity Rapid Fire Sling", *Journal of Propulsion and Power*, Vol. 18, No. 2, March-April 2002

[10]The VLHC Design Study Group, "Design Study for a Staged Very Large Hadron Collider", Fermilab-TM-2149, June, 2001.

[11]S. Ohashi, K. Higashi, H. Ohsaki, and E. Masada, "Influence of magnet quench on the superconducting magnetically levitated bogie," *IEEE Transactions on Magnetics*, vol. 32, pp. 5046—8, September 1996.

[12]Personal communication, Miles Palmer, SAIC, 2004.

[13]G. Wood, "Electronics Manufacturing Improvements For Precision Guided Weapons", *Emphasis*, American Competitiveness Institute, April, 2004

[14]S. S. Kessler, S. M. Spearing, G. A. Kirkos, "Design of a High-g Unmanned Aerial Vehicle Structure", SAE Report 2000-01-5538

[15]R. M. Jones, "Electromagnetically Launched Micro Spacecraft for Space Science Missions", AIAA Paper 88-0068, January, 1988

[16]M. R. Palmer, R. X. Lenard, "A Revolution in Access to Space Through Spinoffs of SDI Technology", IEEE Transactions On Magnetics, Vol. 27, No. 1, January 1991

[17]Automation, Robotics, and Simulation Division (ARSD), NASA Johnson Space Center, Houston, Texas, http://vesuvius.jsc.nasa.gov/er/